Chem. Senses 27: 521–527, 2002

# Cell Death of Olfactory Receptor Neurons in a Rat with Nasosinusitis Infected Artificially with *Staphylococcus*

**Y. Ge[1,2], T. Tsukatani[2], T. Nishimura[2], M. Furukawa[2] and T. Miwa[2]**

[1]People's Hospital of Beijing University, Beijing, China and [2]Kanazawa University Graduate School of Medical Science, Kanazawa City, Japan

*Correspondence to be sent to: Takaki Miwa, Department of Otorhinolaryngology, Kanazawa University Graduate School of Medical Science, Takara Machi 13-1, Kanazawa City, Japan 920-8641. e-mail: miwataka@orl.m.kanazawa-u.ac.jp*

## Abstract

Nasosinusitis is a common cause of acquired hyposmia or anosmia. To study the apoptotic death of olfactory receptor neurons in nasosinusitis, we made an inflammation model in rat infected with *Staphylococcus*. The histochemical changes in olfactory epithelium were examined using antibodies against protein gene product 9.5 (PGP 9.5), single-strand DNA (ssDNA), Bcl-2 and Bax that might be involved in the apoptosis of olfactory receptor neurons. The thickness of olfactory epithelium and the number of ssDNA-labeled cells were evaluated in each post-treatment group and the results were analyzed by two-way analysis of variance (ANOVA) and *post hoc* tests. Hematoxylin–eosin staining showed that a severe inflammatory reaction had occurred on the infected side of the nasal cavity and sinus, but not on the non-infected side. However, apoptosis of olfactory receptor neurons occurred on both sides; the apoptosis on the non-infected side started later and behaved like a shadow curve similarly to the infected side. Repeated measures ANOVA showed significant differences of both the thickness of olfactory epithelium ($P < 0.0001$) and the number of ssDNA-labeled cells ($P = 0.0339$) in the epithelium between the infected side and non-infected side comparing treatment, time and their interactions. Bcl-2 and Bax were detected only on the infected side in the early stages. Thus, nasosinusitis induced the apoptosis of olfactory receptor neurons. However, the apoptosis occurred not only on the infected side, but also on the non-infected side with no significant inflammation. The Bcl-2/Bax family seems to play an important role in the apoptosis induced by infection, but not in the apoptosis on the non-infected side. The results suggest that mechanisms of apoptosis of olfactory receptor neurons on the infected side may differ from those on the non-infected side.

## Introduction

Apoptosis is a programmed gene-regulated cell death in which tissue architecture can be preserved (Oppenheim, 1991). Neuronal apoptosis plays an important role not only in the development of the nerve system, but also in trauma, infection and neurodegenerative disease (Rink *et al*., 1995; Stefanis *et al*., 1997). In mammals, olfactory neurons are renewed through a cyclic process of life and death during the lifespan of the animal. Since the olfactory epithelium is constantly exposed to airborne environmental stresses, the ability to adapt to injury from these insults is essential in maintaining olfactory function. Investigations of apoptosis of olfactory neurons under pathologic conditions are therefore of considerable interest.

Nasosinusitis and head injury are common causes of acquired hyposmia or anosmia. Experiments by Deckner and colleagues (Deckner *et al*., 1997) showed loss of olfactory receptor neurons following olfactory nerve transection in the rat and showed cell death to be due to apoptosis. Nasosinusitis can also cause hyposmia or anosmia due to nasal obstruction; it may also damage olfactory epithelium. Is neuron apoptosis also involved during inflammation? Does olfactory receptor neuron apoptosis occur only in the infected area? Is the mechanism of apoptosis in nasal inflammation the same as in nerve injury?

In this study, we made a nasosinusitis model in rats to answer these questions about the apoptosis of olfactory receptor neurons. Four kinds of primary antibody were used to observe apoptotic change of olfactory neuroepithelium. Protein gene product 9.5 (PGP 9.5) is a neurospecific peptide (Doran *et al*., 1983). Here we used it to show the olfactory receptor neurons (Johnson *et al*., 1995). Single-strand DNA (ssDNA) is the product of apoptosis, which comes from the effect of endonuclease on DNA. This is a new and convenient method to detect *in situ* apoptosis immunohistochemically and has been shown to be effective (Watanabe *et al*. 1999). Bcl-2 is a member of a large gene family of encoding proteins that can either inhibit (e.g. Bcl-2, Bcl-x) or promote (e.g. Bax, Bcl-X, Bak) apoptosis. Bcl-2 is an intracellular membrane protein and resides primarily in the nuclear envelope, outer mitochondrial membrane and

endoplasmic reticulum. Bax also belongs to the Bcl-2 family and is involved in apoptosis under some conditions and can promote cell death. Bax has also been shown to be directly induced by tumor suppressor p53, which is involved in DNA damage. In this study, we used these antibodies to investigate the possible factors involved in apoptosis of olfactory receptor neurons in infection.

## Materials and methods

### Animal experiment

Eight-week-old, male Sprague–Dawley rats, weighing from 260 to 280g, were used in this study. All animals were treated in accordance with the guidelines of the Institutional Committee for Experimental Animals, Kanazawa University Faculty of Medicine.

Animals were divided into seven groups, each of which contained three rats. Animals were killed 1, 3, 7, 14, 21 or 28 days after the treatment described below, and three other animals which did not receive any treatment were killed as the control group.

### Infection procedure

Animals in the treatment group were deeply anesthetized by i.p. injection of sodium pentobarbital (50 mg/kg). An incision was made in the medial side of the left ala to enlarge the nares. A 1 × 2 × 18 mm polyvinyl acetal applicator (Merocel; XOMED Surgical Products, Jacksonville, FL), smeared with *Staphylococcus*, was then inserted into the left nasal cavity. *Staphylococcus aureus* strain 209P was obtained from the Japan Collection of Microorganisms and then cultured for 24 h at 37°C prior to administration. The polyvinyl acetal applicator was left in the nasal cavity until perfusion. The wound was sutured and the animal was allowed to recover from anesthesia before being returned to its cage.

### Histochemistry

For morphological analysis, animals were deeply anesthetized and thoracotomied, then perfused and fixed via the heart. The perfusion solution was 0.01 M phosphate-buffered saline (PBS, pH 7.0) and the fixation solution was 4% paraformaldehyde (PFA)–0.1 M PBS. The nasal part was then dissected and postfixed in 4% PFA–0.1 M PBS overnight, followed by decalcification in 12% EDTA for >2 weeks.

After paraffin embedding, the fixed and decalcified nasal tissues were cut in 1 μm-thick sections and used for hematoxylin–eosin (H–E) staining and immunohistochemical analysis.

In immunohistochemical staining, after deparaffination and rehydration, specimens were subjected to antigen retrieval by microwave in citrate buffer (pH 7.0, 80°C, 20 min) for Bax and Bcl-2, or 0.4% trypsin incubation (room temperature, 10 min) for ssDNA, or both for PGP 9.5. After incubating with 3% $H_2O_2$ and 1% bovine serum albumin/Tris-buffered saline (BSA/TBS) to block endogenous peroxidase and nonspecific reactions, respectively, specimens were incubated with the primary antibodies PGP 9.5 (1:400, DAKO code no. Z5116), ssDNA (1:400, DAKO code no. A4506), Bax (1:800, Pharmingen catalog no. 554106), Bcl-2 (1:800, Pharmingen catalog no. 13456E) at room temperature for ~60 min. EnVision peroxidase (Rabbit, DAKO code no. K4002) was used as the second antibody and 3,3′-diaminobenzidine (DAB, DAKO code no. K3465) was used as the substrate-chromogen system. Color development was monitored under a microscope and ended by rinsing with distilled water. A thorough washing with TBS (pH 7.6) followed each step, except the incubation with 1% BSA/TBS.

Counterstaining with hematoxylin was done for <30 s, followed by rinsing in running water for 15–18 min.

The brain stems of healthy control group rats were used as the positive control for Bcl-2 and Bax according to the manufacturers' instructions and different primary antibodies incubated with consecutive sections were used as the negative control.

### Data analysis

The thickness of the olfactory epithelium and the number of ssDNA-labeled cells were evaluated in three randomly selected olfactory epithelial fields on both sides of the nasal cavity. The number of ssDNA-labeled cells was counted in a 0.25 $mm^2$ area of the olfactory epithelium. Average and standard error (SE) were used to make graphs to show the changes. Results were analyzed by two-way analysis of variance (ANOVA) and *post hoc* tests comparing treatment, time and their interactions.

## Results

The animals showed some general symptoms of inflammation, such as weariness and reduced drinking and eating over the first 3 days. Some rats suffered dyspnea to a certain extent. However, after the day 4, nearly all of the animals seemed to return to normal activities and ate normally.

### Histochemistry

#### *Control group*

In H-E stained tissue sections, the olfactory mucosa showed a structured epithelium, comprised of olfactory neuron receptor cells, supporting cells, basal cells and the duct cells of Bowman's glands. Submucosal structures, including Bowman's glands, olfactory axon bundles and their associated Schwann cells, blood vessels and connective tissue, were also observed.

In PGP 9.5 staining, olfactory neurons and submucosa axon bundles were strongly stained. These neurons showed in an orderly arrangement in about four to eight layers and their dendrites can also be seen clearly between supporting cells. ssDNA staining showed only a few positive cells

dispersed in olfactory epithelium in the normal 8-week-old rats. There was no Bcl-2 or Bax staining detected in the olfactory epithelium in this group (data not shown).

*Nasosinusitis model*

In this model, H–E stained tissue clearly showed sinusitis-related changes on the infected side only (Figure 1A,B), such as inflammatory cell infiltration, vascular dilation and severe luminal exudation. These changes were most prominent on day 1 in both the nasal cavity and the sinus and subsequently declined gradually. The thickness of the olfactory epithelium decreased, beginning on day 1 and reached its thinnest level at about day 14. Nearly no supporting cells were left by day 3, which may have been due to necrosis, and did not begin to recover until day 14. On the other side in the same rat, there was nearly no inflammatory reaction in the olfactory epithelium, but the thickness of the olfactory epithelium was also decreased on day 7 (Figure 1C) compared to control animals and reached a minimum on day 21. The changes of epithelium thickness on both sides are shown in Figure 2. On the infected side, the decrease in thickness of the olfactory epithelium was significant in all the post-treatment days ($P < 0.0001$), while on the non-infected side, the thickness decreased significantly from day 7 ($P < 0.0001$). Repeated measures ANOVA showed significant differences between the infected side and

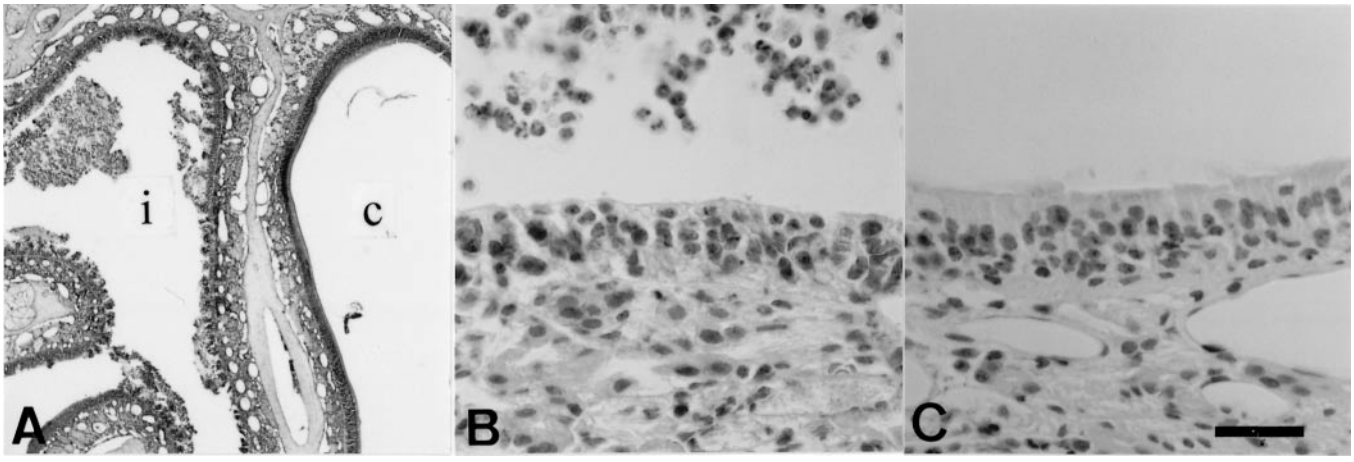


**Figure 1** **(A)** H–E staining on day 1 after treatment. Severe inflammatory reaction is shown on the infected side (i) only. There is no inflammation detected on the control side (c) of the nasal cavity. **(B)** On the infected side on day 7, note the loss of apical cytoplasm of supporting cells and the obviously decreased thickness of olfactory epithelium. **(C)** On the non-infected side, although there is nearly no inflammation reaction, the thickness of olfactory epithelium also decreased on day 7. Scale bars = 180 μm (A) and 20 μm (B, C).

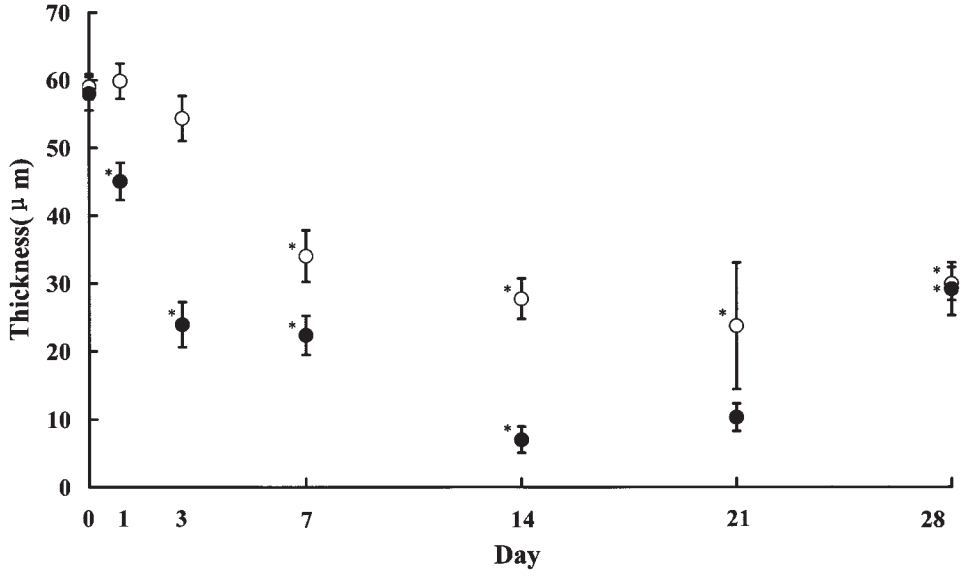


**Figure 2** The change of the thickness of olfactory epithelium. On the infected side (●), the thickness decreased from day 1 and reached its thinnest at about day 14, while on the non-infected side (○), it decreased on day 7 and reached the minimum on day 21. *$P < 0.0001$.

the non-infected side ($P < 0.0001$). Moreover, supporting cells did not decrease until day 14.

With the anti-PGP 9.5 immunohistochemical stain, the layers of positive olfactory neurons decreased from day 1 on the infected side. By day 3, some parts had only the basal cells remaining. Dendrites and cilia of olfactory neurons were also lost in some portions, especially at ~1 week (Figure 3A). By day 28, although the PGP 9.5 positive cells were smaller than normal olfactory cells, some of these small olfactory neurons had regained their dendrites. Supporting cells also diminished in most of the rats and olfactory neurons were then directly exposed to the nasal cavity. The olfactory epithelium on the non-infected side showed nearly normal structure until day 3, while from day 7, the olfactory epithelium became thinner and unstained olfactory neurons, which were located mainly in the deep layers, could be seen clearly on day 14. However, the ciliary structure and orderly arrangement was maintained and most of the supporting cells were still intact (Figure 3B).

Anti-ssDNA positive cells increased from day 1 on the infected side and reached a maximum at day 7 (Figure 4A). By day 21, the number of positive cells was nearly normal.

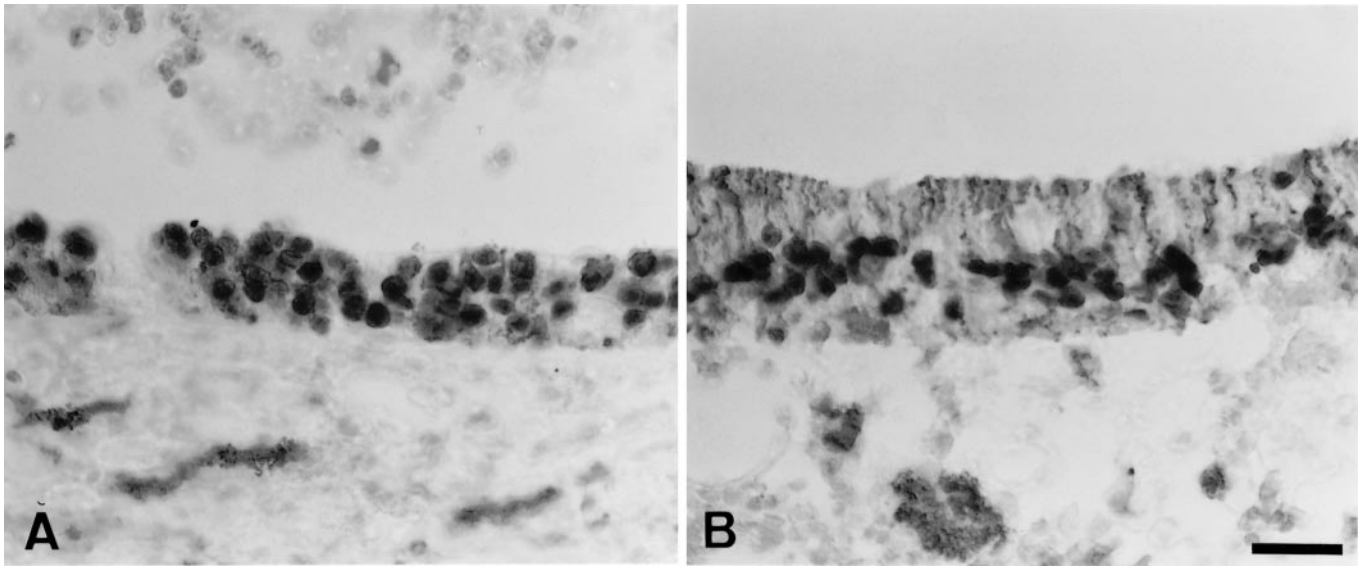


**Figure 3** **(A)** PGP 9.5 immunostaining on the infected side on day 7; the number of positive olfactory neuron has decreased and there are no dendrites. **(B)** PGP 9.5 immunostaining on the non-infected side on day 7; although the number of positive neurons has decreased, the dendrites, ciliary structure and orderly arrangement are still kept well. Calibration bar = 20 μm.

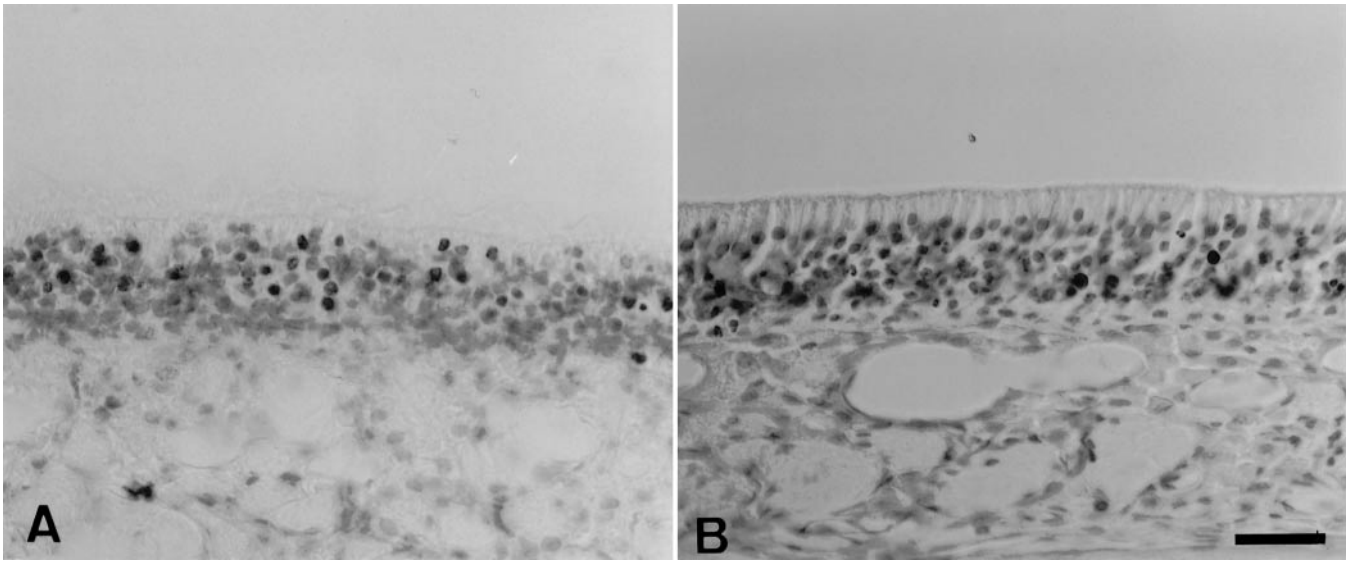


**Figure 4** **(A)** ssDNA immunostaining on the infected side on day 3; there are many positive cells dispersed over the whole epithelium. **(B)** On the non-infected side, the ssDNA positive cells are mainly in the deep part of the olfactory epithelium at the beginning (day 3). Calibration bar = 20 μm.

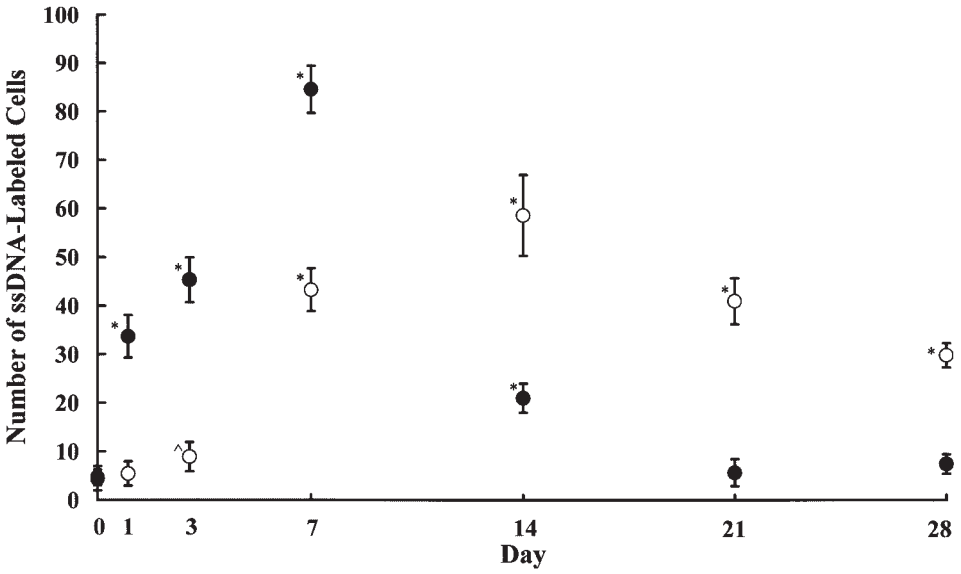


**Figure 5** The number of positive ssDNA cells in olfactory epithelium. On the infected side (●), positive cells increased from day 1 and reached a maximum on day 7; by the 21st day, the number was nearly normal. On the non-infected side (○), apoptosis began to increase from day 3, reached a maximum on day 14 and was still not back to normal by day 28. $^P < 0.01$; $*P < 0.0001$.

On the other side of nasal cavity, apoptosis began to increase in some areas from day 3 (Figure 4B) and reached a maximum at day 14. On day 28, there were still many positive cells on the non-infected side. So the change on the non-infected side looked like a shadow curve of that on the infected side. Figure 5 shows the changes in both sides. On the infected side, the number of ssDNA-labeled cells increased significantly on days 1, 3, 7 and 14 ($P < 0.0001$) compared with control animals. On the non-infected side, ssDNA-labeled cells increased from day 3 ($P < 0.01$), reached a maximum on day 14 and were still not back to normal by day 28 ($P < 0.0001$). Repeated measures ANOVA showed significant differences between the two sides ($P = 0.0339$) comparing treatment, time and their interaction. The curve patterns were also significantly different between the infected and non-infected sides ($P < 0.0001$). The positive cells on the infected side were mainly scattered in the superficial part in the early stage and turned to reach the whole epithelium by day 7 (Figure 4A). On the non-infected side, olfactory neuron apoptosis appeared mainly in the deep part of the olfactory epithelium (Figure 4B).

Bcl-2 expression can be clearly detected in some of the olfactory receptor neurons on days 1 and 3 on the infected side. Some of the positive cells were concentrated on the superficial part of the olfactory epithelium, adjacent to where necrotic changes were detected (Figure 6A). On day 7, there was nearly no expression of Bcl-2. On the other side of the nasal cavity, no positive cells were detected in any groups.

Bax-positive cells were also detected in the early stage of inflammation on the infected side. The positive cells were scattered over some portions and the reaction was not as prominent as Bcl-2 staining (Figure 6B). No positive reaction showed on the non-infected side.

## Discussion

There are several experimental manipulations used to study apoptosis in olfactory receptor neurons: olfactory bulbectomy (Michel *et al.*, 1994); olfactory nerve transection (Simmons *et al.*, 1981); and sensory deprivation by naris occlusion (Farbman *et al.*, 1988). Although previous studies have shown that infection can cause apoptosis of hippocampal neurons (Inja *et al.*, 1997), little is known about apoptosis in olfactory receptor neurons due to nasosinusitis. In this study, we successfully used a delivery system smeared with *Staphylococcus* to make a nasosinusitis model in rat. The results showed that inflammation and substantive olfactory receptor neuron apoptosis occurred during the infection. Farbman's experiment (Farbman *et al.*, 1988) showed that reduction of olfactory neurons started 20 days after naris occlusion for sensory deprivation. In our nasosinusitis model, neuron apoptosis and reduction started within the first 2 weeks. Therefore, we can conclude that the apoptosis reaction in our model may not due to the temporal sensory deprivation effect, but to inflammation.

Infection can damage the structure of the olfactory epithelium and cause olfactory receptor neurons loss. Part of the cell loss is due to necrosis, including both olfactory receptor neurons and supporting cells, and the remaining neurons may also lose part of the dendrites or ciliary structures, as shown in the present experiment. The impairment of neuron structure or intercellular connection may be part of the reason for neuron apoptosis in this model. Inflammation can also produce inflammatory chemokines,

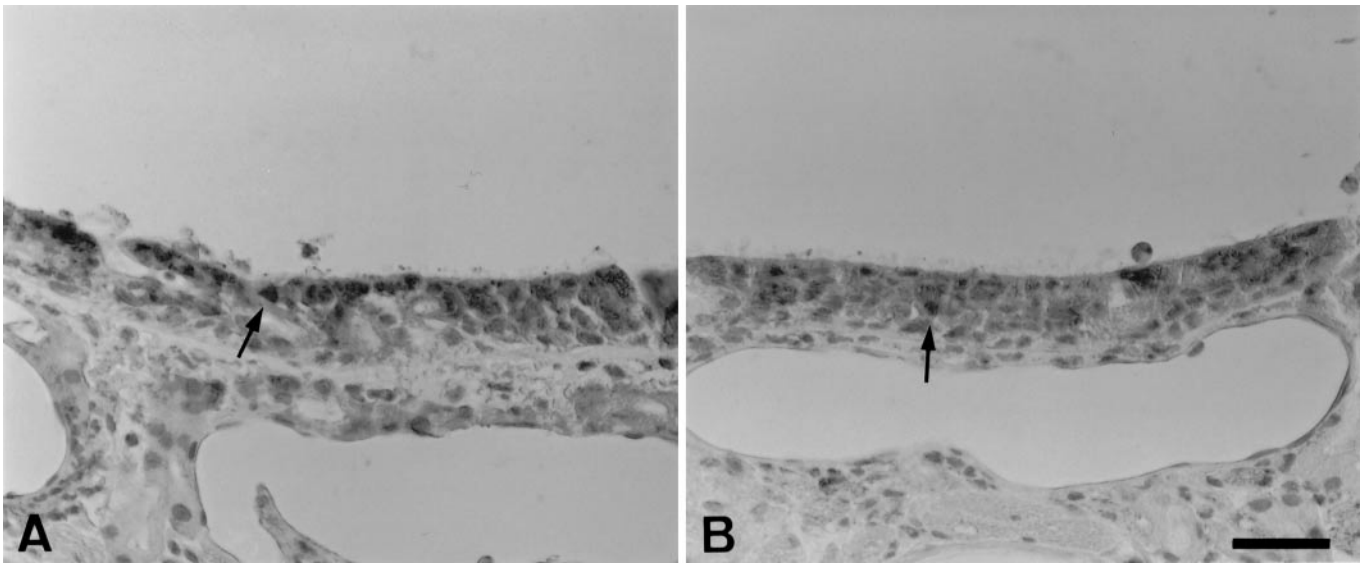


**Figure 6** **(A)** Bcl-2 immunostaining shows many positive neurons (arrow) on the infected side on day 3. The positive cells are located mainly in the superficial part. In the middle layer of the olfactory epithelium, some irregularly arranged cells are seen, which are negative for Bcl-2 and may be due to the necrotic reaction. **(B)** Bax immunostaining shows some positive cells scattered in the olfactory epithelium (arrow). Calibration bar = 20 μm.

such as RANTES, MIP-1α, MCP-1, MCP-3 and IP-10, and cytokines such as TNF-α, IL-1β, IL-6, IL-18 and IFN-α/β, etc. These factors can exaggerate the inflammatory reaction and some of them are ligands that can induce apoptosis by themselves. Earlier experiments (Farbman *et al.*, 1999) have shown that both sets of ligands and receptors, Fas/FasL and TNF-α/TNFR1, were present in olfactory epithelium. So the apoptosis of olfactory receptor neurons during infection may be either a host defense mechanism or may reflect the pathogenesis of the infection. On the one hand, the host is influenced by the inflammatory insult passively and, on the other hand, the organism can eliminate those injured cells actively to maintain normal function.

There are many kinds of mechanisms involved in apoptosis. During the commitment or induction phase of apoptosis, a number of signals cause the cell to enter the apoptotic pathway by altering the balance of proapoptotic and antiapoptotic proteins that determine either susceptibility or resistance to apoptosis. The Bcl-2 family is just one of those modulation proteins. Bcl-2 inhibits apoptosis by preventing the release of apoptosis inducing factor (AIF) and cytochrome C from mitochondria. Bax is a type of factor that can promote cell death. It has been suggested that the tumor suppressor p53 and exposure to DNA-damaging agents could induce Bax release directly. In our experiment, although Bcl-2 was expressed clearly on days 1 and 3 on the infected epithelium, the expression of Bax was scattered and massive olfactory neuron apoptosis followed subsequently and was evident by day 7. The results suggested that apoptosis caused by inflammation might be mediated through a pathway regulated by the Bcl-2 family. However, according to earlier workers (Calof *et al.* 1996), the apoptosis of mature olfactory neurons following bulbectomy was p53 independent and not regulated by Bcl-2. The different expressions of Bcl-2 and Bax suggest that different apoptotic mechanisms are involved in these two situations.

Another interesting finding is the apoptosis of olfactory neurons observed on the non-infected side of the nasal cavity during infection. In our experiment, the sinusitis occurred mainly on the infected side, while the non-infected side showed little inflammatory reaction. However, olfactory receptor neuron apoptosis appeared not only on the infected side, but also on the non-infected side which, though delayed a little compared with the infected side, was followed by a decrease in the thickness of the olfactory epithelium. In contrast to the infected side, the structure of the epithelium on the non-infected side maintained well and there was no positive reaction with either Bcl-2 or Bax. Thus, these responses might indicate active regulation by the organism itself through a different apoptotic pathway from the directly infected area. The physiological and pathological significance of this kind of effect is still not clear, but it seems to be the clinical manifestation of nasosinusitis. It is still unclear if the information or signals are transmitted to other areas by inflammatory media, endotoxins, or the nervous system. Further work should be carried out for a clear understanding of this matter.

## Acknowledgements

We thank Dr T. Tatsutomi for help with the animal experiments. This research was partially supported by Japan China Medical Association.

## References

**Calof, A.L., Hagiwara, N., Holcomb, J.D., Mumm, J.S.** and **Shou, J.** (1996) *Neurogenesis and cell death in olfactory epithelium.* J. Neurobiol., 30, 67–81.

**Deckner, M.L., Risling, M.** and **Frisen, J.** (1997) *Apoptotic death of olfactory sensory neurons in the adult rat*. Exp. Neurol., 143, 132–140.

**Doran, J.F., Jackson, P., Kynoch, P.A.** and **Thompson, R.J.** (1983) *Isolation of PGP 9.5, a new human neuron-specific protein detected by high-resolution two-dimensional electrophoresis.* J. Neurochem., 40, 1542–1547.

**Farbman, A.I., Brunjes, P.C., Rentfro, L., Michas, J.** and **Ritz, S.** (1988) *The effect of unilateral naris occlusion on cell dynamics in the developing rat olfactory epithelium*. J. Neurosci., 8, 3290–3295.

**Farbman, A.I., Buchholz, J.A., Suzuki, Y., Coines, A.** and **Speert, D.** (1999) *A molecular basis of cell death in olfactory epithelium.* J. Comp. Neurol., 414, 306–314.

**Inja, B., Stephen, L.L., Marcelle, B., Lucian, C.** and **Martin, G.T.** (1997) *Tumor necrosis factor-alpha contributes to apoptosis in hippocampal neurons during experimental group B streptococcal meningitis.* J. Infect. Dis., 176, 693–697.

**Johnson, E.W., Eller, P.M.** and **Jafek, B.W.** (1995) *Distribution of OMP-, PGP 9.5- and CaBP-like immunoreactive chemoreceptor neurons in the developing human olfactory epithelium.* Anat. Embryol. (Berl.), 191, 311–317.

**Michel, D., Monyse, E., Bran, G.** and **Jourdan, F.** (1994) *Induction of apoptosis of rat olfactory neuroepithelium by synaptic target ablation.* Neuroreport, 27, 1329–1332.

**Oppenheim, R.W.** (1991) *Cell death during development of the nervous system.* Annu. Rev. Neurosci., 14, 453–501.

**Rink, A., Fung, K.M., Trojanowski, J.Q., Lee, V.M., Neugebauer, E.** and **McIntosh, T.K.** (1995) *Evidence of apoptotic cell death after experimental traumatic brain.* Am. J. Pathol., 147, 1575–1583.

**Simmons, P.A., Rafols, J.A.** and **Getchell, T.V.** (1981) *Ultrastructural changes in olfactory receptor neurons following olfactory nerve section.* J. Comp. Neurol., 197, 237–257.

**Stefanis, L., Burke, R.E.** and **Greene, L.A.** (1997) *Apoptosis in neurodegenerative disorders.* Curr. Opin. Neurol., 10, 299–305.

**Watanabe, I., Toyoda, M., Okuda, J., Tenjo, T., Tanaka, K., Yamamoto, T., Kawasaki, H., Sugiyama, T., Kawarada, Y.** and **Tanigawa, N.** (1999) *Detection of apoptotic cells in human colorectal cancer by two different* in situ *methods: antibody against single-stranded DNA and terminal deoxynucleotidyl transferase-mediated dUTP-biotin nick end-labeling (TUNEL) methods.* Jpn. J. Cancer. Res., 90, 188–193.

*Accepted April 11, 2002*